

# BRAIN COMMUNICATIONS

## $\beta$ -Amyloid discordance of cerebrospinal fluid and positron emission tomography imaging shows distinct spatial tau patterns

Chenyang Jiang,<sup>1</sup> Qingyong Wang,<sup>2</sup> Siwei Xie,<sup>1</sup> Zhicheng Chen,<sup>3</sup> Liping Fu,<sup>4</sup> Qiyu Peng,<sup>1</sup> Ying Liang,<sup>5</sup>  Hongbo Guo,<sup>6</sup> and  Tengfei Guo<sup>1,7</sup> for the Alzheimer's Disease Neuroimaging Initiative\*

\*Data used in preparation of this article were obtained from the Alzheimer's Disease Neuroimaging Initiative (ADNI) database ([adni.loni.usc.edu](http://adni.loni.usc.edu)). As such, the investigators within the ADNI contributed to the design and implementation of ADNI and/or provided data but did not participate in analysis or writing of this report.

A complete listing of ADNI investigators can be found at: [http://adni.loni.usc.edu/wp-content/uploads/how\\_to\\_apply/ADNI\\_Acknowledgement\\_List.pdf](http://adni.loni.usc.edu/wp-content/uploads/how_to_apply/ADNI_Acknowledgement_List.pdf)

Extracellular  $\beta$ -amyloid plaques and intracellular neurofibrillary tau tangles are the primary hallmarks of Alzheimer's disease.  $\beta$ -Amyloid pathology can be directly quantified by positron emission tomography imaging or indirectly by measuring the decrease of cerebrospinal fluid  $\beta$ -amyloid<sub>42</sub>/ $\beta$ -amyloid<sub>40</sub> ratio. Although these two  $\beta$ -amyloid biomarkers may be considered interchangeable, they sometimes show discordance, particularly in early stage of Alzheimer's disease. Individuals with cerebrospinal fluid  $\beta$ -amyloid positive only or  $\beta$ -amyloid positron emission tomography positive only may be at early amyloidosis stage compared to those who are cerebrospinal fluid  $\beta$ -amyloid negative and  $\beta$ -amyloid positron emission tomography negative or cerebrospinal fluid  $\beta$ -amyloid positive and  $\beta$ -amyloid positron emission tomography positive. Besides,  $\beta$ -amyloid pathology may play an initiating role in Alzheimer's disease onset, leading to subsequent tau increases. However, it is still unclear whether individuals with different  $\beta$ -amyloid pathways have distinct spatial patterns of cortical tau tangles in early amyloidosis stage. In this study, we analyzed 238 cognitively unimpaired and 77 mild cognitive impairment individuals with concurrent (interval of acquisition <1 year) <sup>18</sup>F-flortaucipir tau positron emission tomography,  $\beta$ -amyloid (<sup>18</sup>F-florbetapir or <sup>18</sup>F-florbetaben) positron emission tomography and cerebrospinal fluid  $\beta$ -amyloid<sub>42</sub> and  $\beta$ -amyloid<sub>40</sub> and cerebrospinal fluid p-Tau<sub>181</sub> and divided them into four different cerebrospinal fluid/positron emission tomography groups based on the abnormal status of cerebrospinal fluid  $\beta$ -amyloid<sub>42</sub>/ $\beta$ -amyloid<sub>40</sub> (cerebrospinal fluid  $\pm$ ) and  $\beta$ -amyloid positron emission tomography ( $\pm$ ). We determined the cortical regions with significant tau elevations of different cerebrospinal fluid/positron emission tomography groups and investigated the region-wise and voxel-wise associations of tau positron emission tomography images with cerebrospinal fluid  $\beta$ -amyloid<sub>42</sub>/ $\beta$ -amyloid<sub>40</sub>,  $\beta$ -amyloid positron emission tomography and cerebrospinal fluid p-Tau/ $\beta$ -amyloid<sub>40</sub> in early (cerebrospinal fluid positive/positron emission tomography negative and cerebrospinal fluid negative/positron emission tomography positive) and late (cerebrospinal fluid positive/positron emission tomography positive) amyloidosis stages. By compared to the cerebrospinal fluid negative/positron emission tomography negative individuals (Ref) without evidence of tau increase measured by cerebrospinal fluid or positron emission tomography, cerebrospinal fluid positive/positron emission tomography negative individuals showed higher tau in entorhinal but not in Braak<sub>III/IV</sub> and Braak<sub>V/VI</sub>, whereas cerebrospinal fluid negative/positron emission tomography positive individuals had significant tau elevations in Braak<sub>V/VI</sub> but not in entorhinal and Braak<sub>III/IV</sub>. In contrast, cerebrospinal fluid positive/positron emission tomography positive individuals showed significant tau increases in all the cortical regions than the Ref group. The voxel-wise analyses provided further evidence that lower cerebrospinal fluid  $\beta$ -amyloid<sub>42</sub>/ $\beta$ -amyloid<sub>40</sub> was associated with higher tau in entorhinal, whilst higher  $\beta$ -amyloid positron emission tomography was related to higher tau in Braak<sub>V/VI</sub> regions in early amyloidosis stage. Both lower cerebrospinal fluid  $\beta$ -amyloid<sub>42</sub>/ $\beta$ -amyloid<sub>40</sub> and higher  $\beta$ -amyloid

Received October 15, 2021. Revised December 21, 2021. Accepted March 29, 2022. Advance access publication March 31, 2022

© The Author(s) 2022. Published by Oxford University Press on behalf of the Guarantors of Brain.

This is an Open Access article distributed under the terms of the Creative Commons Attribution License (<https://creativecommons.org/licenses/by/4.0/>), which permits unrestricted reuse, distribution, and reproduction in any medium, provided the original work is properly cited.

positron emission tomography were correlated with tau aggregation in all the Braak stages regions in late amyloidosis stage. These findings provide novel insights into the spatial patterns of cortical tau tangles in different amyloidosis stages of Alzheimer's disease, suggesting cerebrospinal fluid  $\beta$ -amyloid and  $\beta$ -amyloid positron emission tomography discordant groups may have distinct characteristics of cortical tau tangles in early amyloidosis stage.

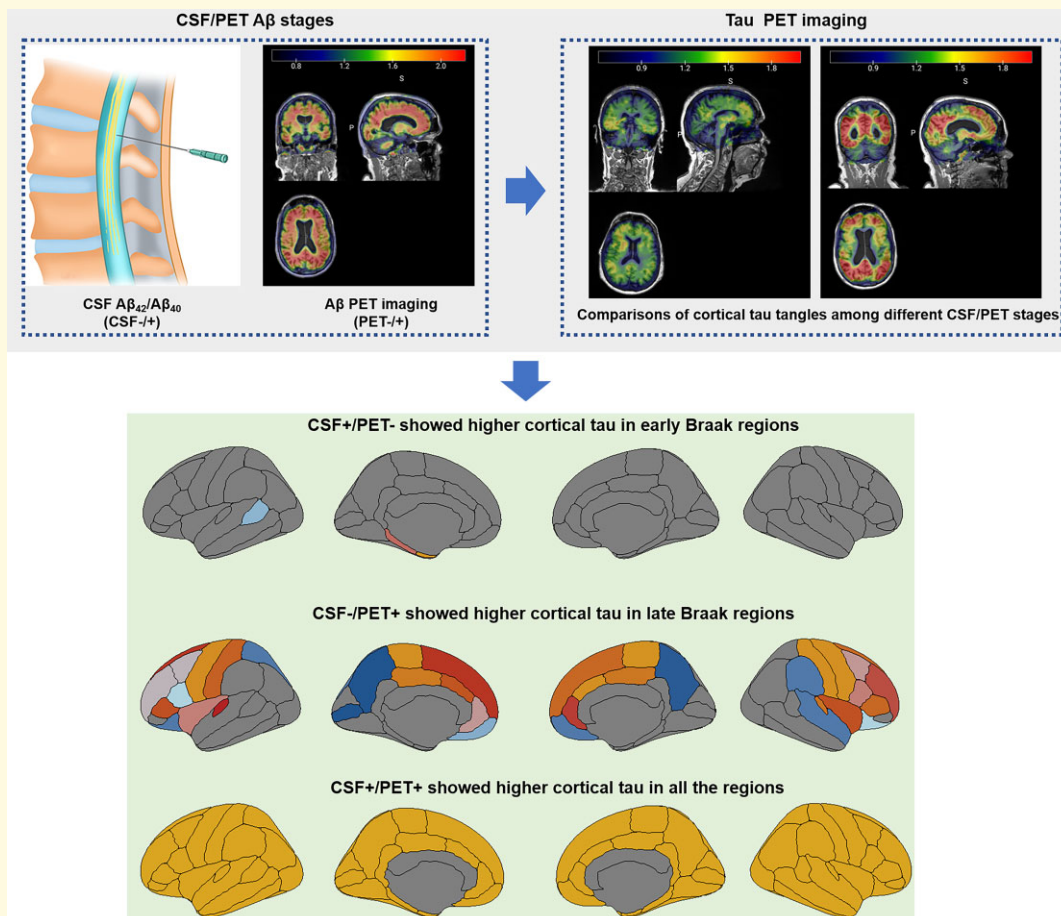
- 1 Institute of Biomedical Engineering, Shenzhen Bay Laboratory, Shenzhen 518132, China
- 2 Department of Neurology, University of Chinese Academy of Sciences-Shenzhen Hospital, Shenzhen 518107, China
- 3 Institute of Chemical Biology, Shenzhen Bay Laboratory, Shenzhen 518132, China
- 4 Department of Nuclear Medicine, China-Japan Friendship Hospital, 2 Yinghuayuan Dongjie, Beijing 100029, China
- 5 Department of Nuclear Medicine, National Cancer Center/National Clinical Research Center for Cancer/Cancer Hospital & Shenzhen Hospital, Chinese Academy of Medical Sciences and Peking Union Medical College, Shenzhen 518116, China
- 6 Department of Neurosurgery, Zhujiang Hospital, Southern Medical University, Guangzhou 510282, China
- 7 Institute of Biomedical Engineering, Peking University Shenzhen Graduate School, Shenzhen 518055, China

Correspondence to: Tengfei Guo, PhD  
 Institute of Biomedical Engineering  
 Shenzhen Bay Laboratory, No.5 Kelian Road  
 Shenzhen 518132, China  
 E-mail: tengfei.guo@szbl.ac.cn

**Keywords:** Alzheimer's disease; cerebrospinal fluid; positron emission tomography imaging;  $\beta$ -amyloid; Tau

**Abbreviations:**  $A\beta$  =  $\beta$ -amyloid; AD = Alzheimer's disease; ADNI = Alzheimer's Disease Neuroimaging Initiative; BANKSSTS = the banks of superior temporal sulcus; CI = confidence interval; CSF = cerebrospinal fluid; CU = cognitively unimpaired; FBB =  $^{18}\text{F}$ -florbetaben; FBP =  $^{18}\text{F}$ -florbetapir; FDR = false discovery rate; FTP =  $^{18}\text{F}$ -flortaucipir; FWE = family wise error; GLM = Generalized Linear Model; IQR = interquartile range; MCI = mild cognitive impairment; PET = positron emission tomography; p-Tau = phosphorylated tau; Ref = reference; ROI = region of interest; SUVR = standardized uptake value ratio

## Graphical Abstract



## Introduction

Extracellular  $\beta$ -amyloid (A $\beta$ ) plaques and intracellular neurofibrillary tau tangles are the primary hallmarks of Alzheimer's disease,<sup>1</sup> and abnormal changes of A $\beta$  pathology have been regarded as the earliest detectable change in Alzheimer's disease.<sup>2,3</sup> A $\beta$  pathology can be qualified *in vivo* by positron emission tomography (PET) imaging<sup>4–6</sup> or indirectly by measuring the decrease of A $\beta$ <sub>42</sub>/A $\beta$ <sub>40</sub> ratio in cerebrospinal fluid (CSF).<sup>7</sup> The concordance and discordance of CSF A $\beta$  and A $\beta$  PET have been investigated cross-sectionally<sup>8–21</sup> and longitudinally.<sup>7,22</sup> Different groups<sup>8,9,13–19,21</sup> have demonstrated that using CSF A $\beta$ <sub>42</sub>/A $\beta$ <sub>40</sub> ratio showed better agreement with A $\beta$  PET than using CSF A $\beta$ <sub>42</sub> alone in different cohorts. Nevertheless, either CSF A $\beta$  (CSF A $\beta$ <sub>42</sub>/A $\beta$ <sub>40</sub> ratio or CSF A $\beta$ <sub>42</sub> alone) or A $\beta$  PET may become abnormal first.<sup>7,13–15,17,22–31</sup> Together our laboratory<sup>7</sup> and other group's findings,<sup>11,22,32</sup> the individuals with CSF A $\beta$  positive only (CSF+/PET–) or A $\beta$  PET positive only (CSF–/PET+) may be at early amyloidosis stage compared to the individuals who are negative (CSF–/PET–) or positive (CSF+/PET+) at both CSF A $\beta$  and A $\beta$  PET. This may represent two different A $\beta$  pathology progressing pathways (pathway1: CSF–/PET–  $\rightarrow$  CSF+/PET–  $\rightarrow$  CSF+/PET+; pathway2: CSF–/PET–  $\rightarrow$  CSF–/PET+  $\rightarrow$  CSF+/PET+). Notably, the 'A $\beta$  pathway' described in this study represents the different A $\beta$  pathology progressing sequences rather than the biological mechanism of A $\beta$  pathology.

Furthermore, A $\beta$  pathology may play an initiating role in Alzheimer's disease onset, leading to subsequent tau increases<sup>6,33,34</sup> or longitudinal tau changes.<sup>3,35–37</sup> The Braak<sub>I–VI</sub> stages<sup>38</sup> have been proposed to characterize the spatial patterns of cortical neurofibrillary tau tangles based on the autopsy data. PET imaging studies<sup>39–43</sup> provide further evidence that the cortical tau tangles may initially present in entorhinal cortex, following by spreading to the Braak<sub>III/IV</sub> and Braak<sub>V/VI</sub> cortical regions in the presence of substantial A $\beta$  burden. However, it is still unclear whether individuals who are on the Alzheimer's continuum but with different A $\beta$  pathways have distinct spatial patterns of cortical tau aggregation. Exploring the spatial distribution of cortical tau tangles is important for understanding the characteristics of Alzheimer's disease pathophysiology in different stages and may provide novel reference for designing anti-tau clinical trials of Alzheimer's disease.

In this study, we analyzed non-demented Alzheimer's Disease Neuroimaging Initiative (ADNI) participants who had concurrent (within 1 year) CSF A $\beta$ <sub>42</sub>/A $\beta$ <sub>40</sub>, phosphorylated tau (p-Tau), A $\beta$  PET and tau PET data and divided them into four different CSF/PET amyloidosis stages based on the abnormal status of CSF A $\beta$ <sub>42</sub>/A $\beta$ <sub>40</sub> and A $\beta$  PET. In order to explore the spatial patterns of cortical tau tangles in different amyloidosis stages, we determined the cortical regions with significant tau elevation of different CSF/PET A $\beta$  stages and investigated the region-wise and voxel-wise associations of tau PET images with CSF A $\beta$ <sub>42</sub>/A $\beta$ <sub>40</sub>, A $\beta$  PET

and CSF p-Tau/A $\beta$ <sub>40</sub> in early (CSF+/PET– and CSF–/PET+) and late (CSF+/PET+) amyloidosis stages.

## Materials and methods

### Participants

The data were obtained from the ADNI database (ida.loni.usc.edu). The ADNI study was approved by institutional review boards of all participating centres, and written informed consent was obtained from all participants or their authorized representatives. In this study, we identified 238 cognitively unimpaired (CU) and 77 mild cognitive impairment (MCI) ADNI participants with concurrent (interval of acquisition <1 year) <sup>18</sup>F-flortaucipir (FTP) tau PET, amyloid [<sup>18</sup>F-florbetapir (FBP) or <sup>18</sup>F-florbetaben (FBB)] PET, CSF A $\beta$ <sub>42</sub> and A $\beta$ <sub>40</sub> and CSF p-Tau. We divided these 315 participants into four CSF/PET groups according to A $\beta$  positivity defined by the thresholds of CSF A $\beta$ <sub>42</sub>/A $\beta$ <sub>40</sub> and A $\beta$  PET as described below: CSF–/PET– (concordant A $\beta$  negative), CSF+/PET– (discordant CSF A $\beta$  positive), CSF–/PET+ (discordant A $\beta$  PET positive) and CSF+/PET+ (concordant A $\beta$  positive). In order to control for the influence of non-Alzheimer's related tauopathy, 43 CSF–/PET– participants with either abnormal CSF p-Tau/A $\beta$ <sub>40</sub><sup>36</sup> or abnormal FTP tau PET (entorhinal or Temporal-metaROI<sup>44</sup>) were excluded from the CSF–/PET– group, and the rest of the CSF–/PET– group were defined as the reference (Ref) group.

### PET imaging and analysis

PET data were acquired in 5-min frames from 50 to 70 min (FBP), 90–110 min (FBB) and 75–105 min (FTP) post-injection, and more details are given elsewhere (<http://adni-info.org>). As described previously,<sup>3</sup> FBP or FBB scans were coregistered to their corresponding baseline structural MRI scans. FreeSurfer (V5.3.0; <https://surfer.nmr.mgh.harvard.edu/>) was used to extract cortical A $\beta$  tracer retention in 68 regions of interest (ROIs) defined by Desikan–Killiany atlas,<sup>45</sup> and FBP or FBB standardized uptake value ratios (SUVRs) were calculated by referring regional florbetapir or florbetaben to that found in the whole cerebellum. A cortical summary COMPOSITE SUVR was created from a COMPOSITE cortical area, including frontal, cingulate, parietal and temporal regions.<sup>46</sup>

The FBB A $\beta$  positivity of the COMPOSITE region was defined as SUVR  $\geq$  1.08, and FBP A $\beta$  positivity of the COMPOSITE region was defined as SUVR  $\geq$  1.11. Finally, FBP and FBB SUVRs were converted to Centiloids using the equations Centiloid = (196.9  $\times$  SUVR<sub>FBP</sub>) – 196.03 and Centiloid = (159.08  $\times$  SUVR<sub>FBB</sub>) – 151.65.

FTP tau PET scans of 5 minutes  $\times$  4 frames were realigned, averaged and registered to the baseline MRI scan that was closest in time to the baseline FTP scan. FTP uptakes in 68 cortical ROIs defined by Desikan–Killiany atlas<sup>45</sup> were

extracted in native FTP tau PET space, and one composite Temporal-metaROI<sup>44</sup> (including entorhinal, parahippocampal, fusiform, amygdala, inferior temporal and middle temporal) FTP SUVR was calculated by referring to a mean inferior cerebellar grey matter uptake.<sup>47</sup> In order to evaluate tau deposition in different Braak neurofibrillary tau stages,<sup>38</sup> we also calculated mean FTP SUVRs in Braak<sub>III/IV</sub> and Braak<sub>IV/VI</sub> that correspond to anatomical definitions of Braak stage III/IV (temporal/limbic) and V/VI (neocortical).<sup>39</sup> The thresholds of entorhinal FTP SUVR and Temporal-meta ROI FTP SUVR were set as  $\geq 1.21$  and  $\geq 1.25$  respectively according to an ROC analysis using the Youden index classifying 280 A $\beta$ - ADNI CU participants and 183 A $\beta$ + ADNI MCI and Alzheimer's disease patients as the endpoint as described previously<sup>36</sup> and also in [supplemental material \(Supplemental Figs. 1–4\)](#).

For the voxel-wise analyses, FTP PET images were spatially normalized to the MNI space, intensity normalized at the voxel-wise level by a mean inferior cerebellar grey matter uptake<sup>47</sup> and smoothed using a Gaussian kernel of 8 mm in SPM12 (Wellcome Department of Imaging Neuroscience, London, UK).

## CSF biomarkers

CSF A $\beta$ <sub>40</sub>, A $\beta$ <sub>42</sub> and p-Tau<sub>181</sub> data were analyzed by the University of Pennsylvania ADNI Biomarker core laboratory using the fully automated Roche Elecsys and cobas e 601 immuno-assay analyzer system. CSF data (UPENN-BIOMK10\_07\_29\_19.csv) were downloaded from the ADNI website. Considering that using a CSF p-Tau/A $\beta$ <sub>40</sub> ratio may reduce measurement error likely related to individual differences in CSF production rather than pathology, and improve associations with AD biomarkers compared to using CSF p-Tau alone,<sup>36</sup> we decided to use CSF p-Tau/A $\beta$ <sub>40</sub> ratio to represent CSF tau in this study. The CSF A $\beta$ <sub>42</sub>/A $\beta$ <sub>40</sub> ratio and CSF p-Tau/A $\beta$ <sub>40</sub> ratio<sup>36</sup> were calculated, and their thresholds were defined as  $\leq 0.054$  and  $\geq 0.0012$  respectively according to the ROC analysis using the Youden index classifying 181 A $\beta$ - CU participants and 163 A $\beta$ + cognitively impaired participants (MCI and Alzheimer's disease patients) as the endpoint as described in [supplemental material \(Supplemental Figs. 5–8\)](#).

## Statistical analysis

Normality of distributions was tested using the Shapiro-Wilk test and visual inspection of data histograms. Data are presented as median (interquartile range [IQR]) or number and percentage. Different CSF/PET groups were compared using a Mann-Whitney U test for continuous characteristics unless otherwise noted. We assessed categorical differences using Fisher's exact test. A false discovery rate (FDR) of 0.05 using Benjamini-Hochberg approach was employed for multi comparisons correction.

In order to investigate tau elevations of different CSF/PET groups, we used generalized linear model (GLM) to compare

FTP SUVRs in 68 FreeSurfer-defined ROIs of CSF+/PET-, CSF-/PET+ and CSF+/PET+ groups with the Ref group (CSF-/PET- without evidence of elevated tau measured by either CSF or PET), controlling for age and sex. We also compared entorhinal FTP SUVR, Braak<sub>III/IV</sub> FTP SUVR, Braak<sub>V/VI</sub> FTP SUVR of different CSF/PET groups with the Ref group.

In addition, the voxel-wise FTP PET images of the CSF+/PET-, CSF-/PET+ and CSF+/PET+ groups were compared with the Ref group using two-sample *t*-test in SPM12, controlling for age and sex. The voxel-wise comparison between the CSF+/PET- group and the Ref group was presented using an uncorrected voxel threshold of  $P < 0.001$ , whilst the other comparisons were presented using an uncorrected voxel threshold of  $P < 0.001$  and with family-wise error (FWE) corrected  $P < 0.05$  at the cluster level.

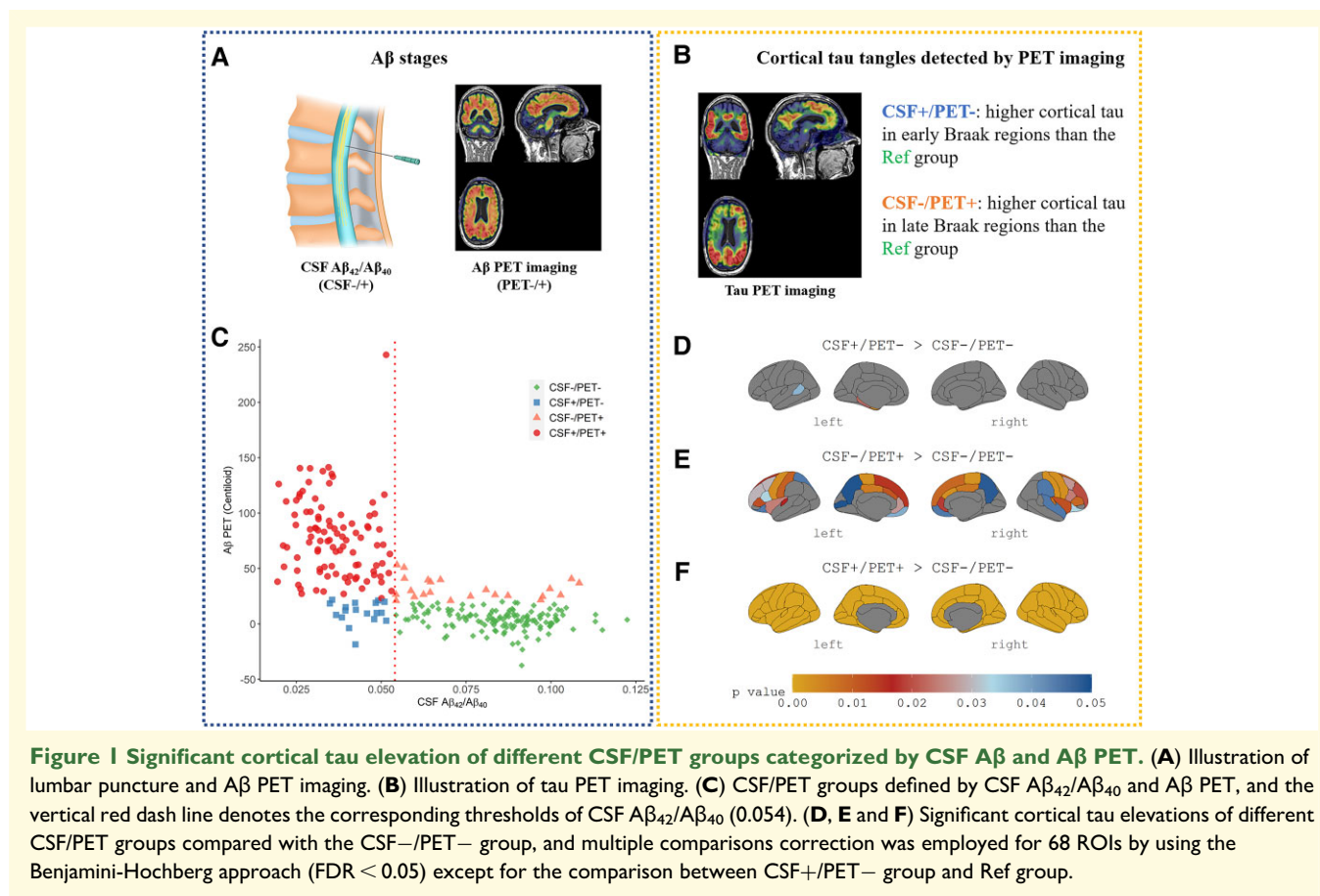
As we described previously,<sup>7</sup> both CSF+/PET- group and CSF-/PET+ group were defined as early amyloidosis stage whilst CSF+/PET+ individuals as late amyloidosis stage of Alzheimer's disease. In order to determine the associations of different A $\beta$  biomarkers as well as CSF p-Tau/A $\beta$ <sub>40</sub> with cortical tau deposition of different Braak stages (entorhinal, Braak<sub>III/IV</sub>, and Braak<sub>V/VI</sub>) cortical regions in different amyloidosis stages, we used GLM model to investigate the association of FTP SUVRs in entorhinal, Braak<sub>III/IV</sub> and Braak<sub>V/VI</sub> with CSF A $\beta$ <sub>42</sub>/A $\beta$ <sub>40</sub>, A $\beta$  PET and CSF p-Tau/A $\beta$ <sub>40</sub> in early (CSF+/PET- and CSF-/PET+ groups and including the CSF-/PET- group as the reference) and late (CSF+/PET+ group and including the CSF-/PET- group as the reference) amyloidosis stages separately, controlling for age and sex. We also investigated the voxel-wise association of FTP PET images with CSF A $\beta$ <sub>42</sub>/A $\beta$ <sub>40</sub>, A $\beta$  PET and CSF p-Tau/A $\beta$ <sub>40</sub> in early and late amyloidosis stages separately, controlling for age and sex. The voxel-wise association between FTP SUVR images and CSF A $\beta$ <sub>42</sub>/A $\beta$ <sub>40</sub> in early amyloidosis stage was presented using an uncorrected voxel threshold of  $P < 0.005$ , whilst the other comparisons were presented using an uncorrected voxel threshold of  $P < 0.001$  and with FWE corrected  $P < 0.05$  at the cluster level.

We noticed that one CSF+/PET- individual and one CSF+/PET+ individual had extremely high entorhinal FTP SUVRs; thus, we repeated all the analyses after removing them from the dataset. In addition, in order to control for the influence of those individuals around the thresholds of CSF A $\beta$ <sub>42</sub>/A $\beta$ <sub>40</sub> and A $\beta$  PET SUVR, we also repeated all the analyses after excluding the borderline participants who were within  $\pm 5\%$  of the CSF A $\beta$ <sub>42</sub>/A $\beta$ <sub>40</sub> and A $\beta$  PET (SUVR) thresholds.

Statistical analyses were performed in the statistical programme R (v3.6.2, The R Foundation for Statistical Computing) unless otherwise noted.

## Data availability

All data used in the current study were obtained from the ADNI database (available at <https://adni.loni.usc.edu>).



## Results

### Demographics

The characteristics of the participants analyzed in this study can be found in [Table 1](#). The majority were CSF-/PET- (Ref group) individuals (49.3%), with the second largest group CSF+/PET+ individuals (35.6%). The discordant groups CSF+/PET- individuals (6.6%) and CSF-/PET+ individuals (8.5%) had similar proportion. The CSF+/PET+ individuals had significantly older age, higher percentages of APOE  $\epsilon 4$  carriers and MCI participants, lower CSF A $\beta_{42}/A\beta_{40}$ , higher A $\beta$  PET Centiloids and larger CSF p-Tau/A $\beta_{40}$  than all the other groups. The CSF-/PET+ group had significantly older age than the Ref group as well. Both CSF+/PET- and CSF-/PET+ individuals had significantly lower CSF A $\beta_{42}/A\beta_{40}$  ratio, higher A $\beta$  PET Centiloids and larger CSF p-Tau/A $\beta_{40}$  ratio than the Ref group.

### Cortical tau elevations of different CSF/PET groups

As shown in [Fig. 1](#), the CSF+/PET- group had significantly higher tau deposition in the left entorhinal and parahippocampal than the CSF-/PET- (Ref) group, and also in the

left banks of superior temporal sulcus (BANKSSTS) although the effect size ( $t=2.09$ ,  $P=0.037$ ) was limited. In contrast, the CSF-/PET+ group showed significant tau increases in a few ROIs in Braak<sub>IV</sub> stage (bilateral caudal anterior cingulate, rostral anterior cingulate, posterior cingulate, insula) and most of the ROIs in Braak<sub>V/VI</sub> stage (except for frontal pole, pars orbitalis, lateral occipital, inferior parietal, BANKSSTS and cuneus) than the Ref group. The CSF+/PET+ group had significant tau elevation in all the cortical regions than the Ref group.

### Comparisons of tau deposition amongst different CSF/PET groups

As illustrated in [Fig. 2](#), the CSF+/PET- group had higher FTP SUVR in entorhinal (estimate = 0.10 [95% confidence interval (CI), 0.023 to 0.179],  $P=0.012$ ) but not in Braak<sub>III/IV</sub> and Braak<sub>V/VI</sub> than the Ref group. In contrast, the CSF-/PET+ group showed higher FTP SUVR in Braak<sub>V/VI</sub> FTP SUVR (estimate = 0.069 [95% CI, 0.023 to 0.115],  $P=0.004$ ) but not in entorhinal and Braak<sub>III/IV</sub> than the Ref group. The CSF+/PET+ group had higher FTP SUVR in entorhinal (estimate = 0.26 [95% CI, 0.219 to 0.305],  $P<0.001$ ), Braak<sub>III/IV</sub> (estimate = 0.176 [95% CI, 0.136 to 0.215],  $P<0.001$ ) and Braak<sub>V/VI</sub> FTP SUVR

**Table 1** Demographic characteristics of participants in different CSF/PET groups

CSF/PET groups	Ref CSF-/PET-	Early amyloidosis		Late amyloidosis CSF+/PET+
		CSF+/PET-	CSF-/PET+	
Participants, n (%)	134 (49.3)	18 (6.6)	23 (8.5)	97 (35.6)
MCI, n (%)	26 (19.4)	6 (33.3)	2 (8.7)	<b>43 (44.3)<sup>a</sup></b>
Age (years)	69.6 (8.8)	70.7 (14.9)	<b>72.5 (7.3)<sup>b</sup></b>	<b>75.1 (10.5)<sup>c</sup></b>
Sex, female, n (%)	86 (64.2)	8 (44.4)	13 (56.5)	56 (57.7)
APOE-ε4, n (%)	31 (23.1)	8 (44.4)	7 (30.4)	<b>64 (66.0)<sup>d</sup></b>
Education (years)	17.5 (2.0)	18.0 (2.0)	16.0 (3.0)	16.0 (4.0)
CSF Aβ <sub>42</sub> /Aβ <sub>40</sub> ratio	0.09 (0.01)	<b>0.04 (0.01)<sup>e,h</sup></b>	<b>0.07 (0.03)<sup>f</sup></b>	<b>0.03 (0.01)<sup>g,i,j</sup></b>
Aβ PET Centiloids	4.44 (10.28)	<b>11.0 (12.49)<sup>k</sup></b>	<b>28.4 (13.6)<sup>l,n</sup></b>	<b>74.9 (49.5)<sup>m,o,p</sup></b>
CSF p-Tau/Aβ <sub>40</sub> ratio	0.0009 (0.0002)	<b>0.0012 (0.0003)<sup>q</sup></b>	<b>0.0010 (0.0002)<sup>r,t</sup></b>	<b>0.0017 (0.0008)<sup>s,u,v</sup></b>

<sup>a</sup>Percentage of MCI: CSF+/PET+ > CSF-/PET-: estimate = 3.29 [95% CI: 1.77, 6.22],  $P < 0.001$ ; CSF+/PET+ > CSF-/PET+: estimate = 8.25 [95% CI: 1.85, 76.4],  $P < 0.01$ , Mann-Whitney U test.

<sup>b</sup>Age: CSF-/PET+ > CSF-/PET-: estimate = 3.41 [95% CI: 0.63, 5.97],  $P = 0.048$ .

<sup>c</sup>CSF+/PET+ > CSF-/PET-: estimate = 4.61 [95% CI: 2.62, 6.65],  $P < 0.001$ , Mann-Whitney U test.

<sup>d</sup>Percentage of APOE-ε4 Carriers: CSF+/PET+ > CSF-/PET-: odds ratio = 6.38 [95% CI 3.47, 12.0],  $P < 0.001$ ; CSF+/PET+ > CSF-/PET+: odds ratio = 4.37 [95% CI 1.52, 13.9],  $P = 0.012$ . Fisher exact test.

<sup>e</sup>CSF Aβ<sub>42</sub>/Aβ<sub>40</sub> ratio: CSF+/PET- < CSF-/PET-: estimate = -0.042 [-0.048, -0.037],  $P < 0.001$ .

<sup>f</sup>CSF-/PET+ < CSF-/PET-: estimate = -0.02 [-0.020, -0.002],  $P < 0.014$ .

<sup>g</sup>CSF+/PET+ < CSF-/PET-: estimate = -0.049 [-0.053, -0.046],  $P < 0.001$ .

<sup>h</sup>CSF+/PET- < CSF-/PET+: estimate = -0.026 [-0.041, -0.018],  $P < 0.001$ .

<sup>i</sup>CSF+/PET+ < CSF+/PET-: estimate = -0.007 [-0.012, -0.003],  $P = 0.001$ .

<sup>j</sup>CSF+/PET+ < CSF-/PET+: estimate = -0.035 [-0.045, -0.029],  $P < 0.001$ ; Mann-Whitney U test.

<sup>k</sup>Aβ PET Centiloids: CSF+/PET- > CSF-/PET-: estimate = 6.93 [2.61, 11.4],  $P = 0.002$ .

<sup>l</sup>CSF-/PET+ > CSF-/PET-: estimate = 26.2 [22.3, 30.8],  $P < 0.001$ .

<sup>m</sup>CSF+/PET+ > CSF-/PET-: estimate = 70.8 [64.0, 77.5],  $P < 0.001$ .

<sup>n</sup>CSF-/PET+ > CSF+/PET-: estimate = 19.0 [13.9, 25.7],  $P < 0.001$ .

<sup>o</sup>CSF+/PET+ > CSF+/PET-: estimate = 64.7 [50.1, 70.0],  $P < 0.001$ .

<sup>p</sup>CSF+/PET+ > CSF-/PET+: estimate = 44.0 [29.0, 55.3],  $P < 0.001$ ; Mann-Whitney U test.

<sup>q</sup>CSF p-Tau/Aβ<sub>40</sub> ratio: CSF+/PET- > CSF-/PET-: estimate = 0.0003 [0.0002, 0.0004],  $P < 0.001$ .

<sup>r</sup>CSF-/PET+ > CSF-/PET-: estimate = 0.0001 [0.0000, 0.0002],  $P < 0.012$ .

<sup>s</sup>CSF+/PET+ > CSF-/PET-: estimate = 0.0007 [0.0006, 0.0008],  $P < 0.001$ .

<sup>t</sup>CSF+/PET- > CSF-/PET+: estimate = 0.0002 [0.0000, 0.0003],  $P = 0.003$ .

<sup>u</sup>CSF+/PET+ > CSF+/PET-: estimate = 0.0005 [0.0002, 0.0006],  $P < 0.001$ .

<sup>v</sup>CSF+/PET+ > CSF-/PET+: estimate = 0.0007 [0.0005, 0.0008],  $P < 0.001$ .

(estimate = 0.122 [95% CI, 0.094 to 0.149],  $P < 0.001$ ) than the Ref group.

In the voxel-wise analysis, the CSF+/PET- group showed higher tau PET in the left entorhinal cortex and parahippocampal (Fig. 2D,  $P < 0.001$  without cluster correction) than the Ref group, whereas the CSF-/PET+ group showed significant increases of FTP SUVRs in Braak<sub>IV</sub> stage ROIs (bilateral caudal anterior cingulate, rostral anterior cingulate, insula, posterior cingulate and isthmus cingulate) and most of the Braak<sub>V/VI</sub> stage ROIs (bilateral medial orbitofrontal, caudal middle frontal, rostral middle frontal, superior temporal, precuneus, postcentral, superior frontal, precentral and paracentral) (Fig. 2E,  $P < 0.001$  with FWE  $P < 0.05$  cluster correction). In addition, the CSF+/PET+ group showed significant (Fig. 2F,  $P < 0.001$  with FWE cluster correction) elevated tau in most of the cortical regions except for pericalcarine and cuneus.

After removing two individuals with extremely high entorhinal FTP SUVRs, the CSF+/PET- group still had significantly higher tau deposition in the left entorhinal than the Ref group, and the results of other comparisons were substantially the same (Supplemental Fig. 9). Besides, the two discordant groups also showed distinct spatial cortical tau deposition, whilst we removed the individuals who were

within  $\pm 5\%$  of the CSF Aβ<sub>42</sub>/Aβ<sub>40</sub> and Aβ PET thresholds (Supplemental Fig. 14), although more cortical regions (left entorhinal, parahippocampal, fusiform, inferior temporal, middle temporal, superior temporal and BANKSSTS) showed significant tau increases in CSF+/PET- group compared to the Ref group (Supplemental Fig. 15).

## Associations of cortical tau with CSF biomarkers and Aβ PET in early and late amyloidosis stages

In early amyloidosis stage, lower CSF Aβ<sub>42</sub>/Aβ<sub>40</sub> was associated with higher FTP SUVR in entorhinal (standardized  $\beta$  ( $\beta_{std}$ ) -0.22 [95% CI, -0.37 to -0.07],  $P = 0.004$ ) but not in Braak<sub>III/IV</sub> and Braak<sub>V/VI</sub> (Fig. 3A, D and G), whereas higher Aβ PET was related to higher FTP SUVR in Braak<sub>III/IV</sub> (Fig. 3E,  $\beta_{std} = 0.24$  [95% CI, 0.09 to 0.38],  $P = 0.002$ ) and Braak<sub>V/VI</sub> (Fig. 3H,  $\beta_{std} = 0.35$  [95% CI, 0.22 to 0.49],  $P < 0.001$ ) but not in entorhinal cortex. However, we found positive association between CSF p-Tau/Aβ<sub>40</sub> and tau PET in entorhinal, Braak<sub>III/IV</sub> and Braak<sub>V/VI</sub> (Fig. 3C, F and I).

In late amyloidosis stage, lower CSF Aβ<sub>42</sub>/Aβ<sub>40</sub> was negatively related to higher FTP SUVR in entorhinal

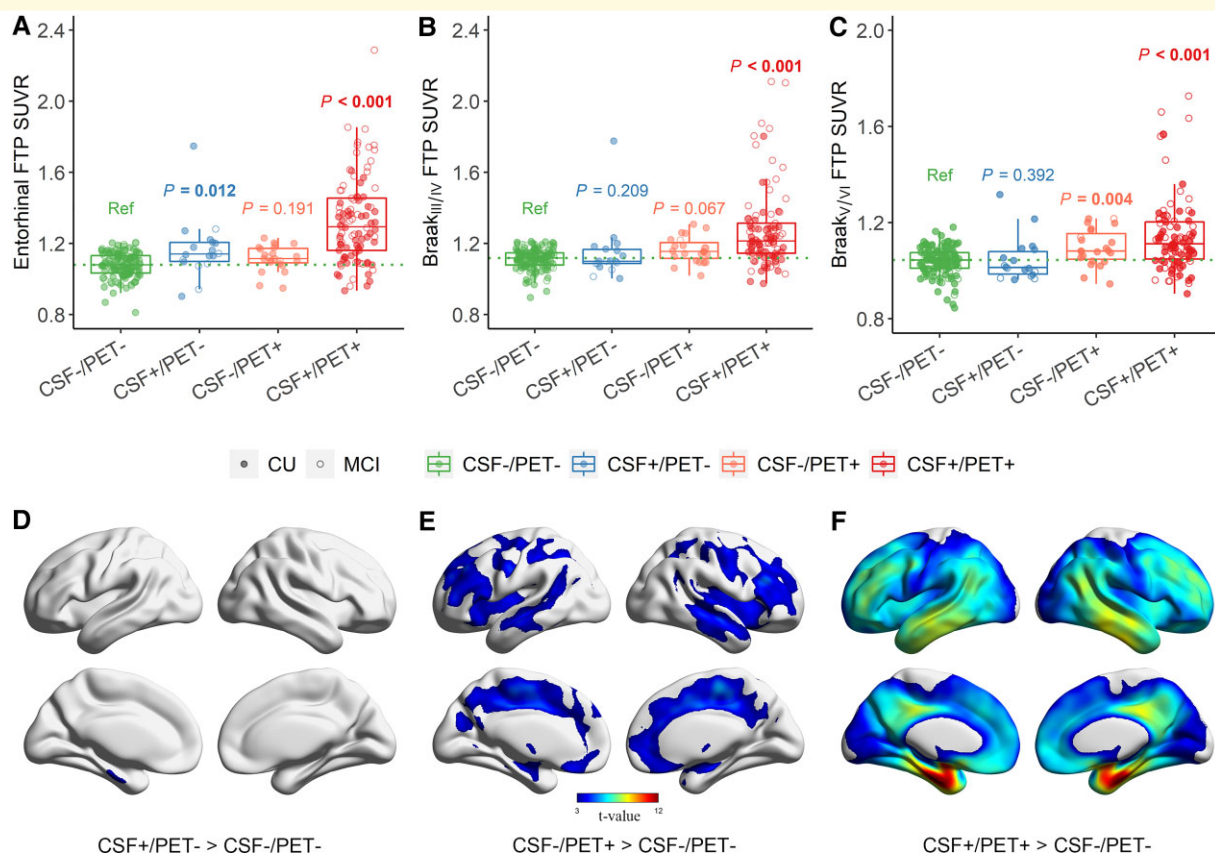


**Figure 2 Comparisons of cortical tau deposition among different CSF/PET groups.** Comparison of FTP SUVRs in (A) entorhinal, (B) Braak<sub>III/IV</sub> and (C) Braak<sub>V/VI</sub> among different CSF/PET groups. The boxplot whiskers extend to the lowest and highest data points within 1.5 times the IQR, from the lower and upper quartiles. The dots represent individual points of each CSF/PET group. Green dashed lines represent the median values of the reference (Ref) group. Values at the top of the bar indicate the  $P$  values of the comparisons with the Ref group. Voxel-wise comparisons of tau PET images of (D) CSF+/PET-, (E) CSF-/PET+ and (F) CSF+/PET+ with the Ref group. Two-sample  $t$ -tests, the comparison between CSF+/PET- group, and the Ref group was presented by using a threshold  $P < 0.001$  at the voxel level, whilst the other comparisons were presented by using a threshold  $P < 0.001$  at the voxel level and with FWE corrected  $P < 0.05$  at the cluster level.

(Fig. 4A,  $\beta_{\text{std}} = -0.60$  [95% CI,  $-0.71$  to  $-0.49$ ],  $P < 0.001$ ), Braak<sub>III/IV</sub> (Fig. 4D,  $\beta_{\text{std}} = -0.48$  [95% CI,  $-0.59$  to  $-0.36$ ],  $P < 0.001$ ) and Braak<sub>V/VI</sub> (Fig. 4G,  $\beta_{\text{std}} = -0.45$  [95% CI,  $-0.57$  to  $-0.33$ ],  $P < 0.001$ ). Higher A $\beta$  PET was positively related to higher FTP SUVR in entorhinal (Fig. 4B,  $\beta_{\text{std}} = 0.66$  [95% CI,  $0.55$  to  $0.76$ ],  $P < 0.001$ ), Braak<sub>III/IV</sub> (Fig. 4E,  $\beta_{\text{std}} = 0.54$  [95% CI,  $0.43$  to  $0.66$ ],  $P < 0.001$ ) and Braak<sub>V/VI</sub> FTP SUVR (Fig. 4H,  $\beta_{\text{std}} = 0.54$  [95% CI,  $0.42$  to  $0.65$ ],  $P < 0.001$ ). Higher CSF p-Tau/A $\beta_{40}$  was positively associated with higher FTP SUVR in entorhinal (Fig. 4C,  $\beta_{\text{std}} = 0.73$  [95% CI,  $0.63$  to  $0.83$ ],  $P < 0.001$ ), Braak<sub>III/IV</sub> (Fig. 4F,  $\beta_{\text{std}} = 0.75$  [95% CI,  $0.66$  to  $0.84$ ],  $P < 0.001$ ) and Braak<sub>V/VI</sub> (Fig. 4I,  $\beta_{\text{std}} = 0.69$  [95% CI,  $0.59$  to  $0.79$ ],  $P < 0.001$ ).

After removing two individuals with extremely high entorhinal FTP SUVR, the significant association between tau PET and CSF p-Tau/A $\beta_{40}$  in early amyloidosis stage disappeared, whilst the other associations retained (Supplemental Figs. 11 and 12). Besides, the results were substantially the same whilst we removed the borderline individuals (Supplemental Figs. 17 and 18).

## Voxel-wise analysis of cortical tau with CSF biomarkers and A $\beta$ PET in early and late amyloidosis stages

In early amyloidosis stage, lower CSF A $\beta_{42}$ /A $\beta_{40}$  was significantly associated with higher FTP SUVR in the left entorhinal cortex (Fig. 5A), higher A $\beta$  PET Centiloid was significantly related to higher FTP SUVRs in right insula and bilateral cingulate cortex, paracentral, frontal and parietal cortices (Fig. 5C), and CSF p-Tau/A $\beta_{40}$  showed significant positive association with FTP SUVRs in left entorhinal, parahippocampal, fusiform, inferior temporal, middle temporal and BANKSSTS (Fig. 5E). In contrast, CSF A $\beta_{42}$ /A $\beta_{40}$ , A $\beta$  PET and CSF p-Tau/A $\beta_{40}$  all showed significant relation with FTP SUVRs in all the Braak ROIs, and the strongest association was found between FTP SUVR and CSF p-Tau/A $\beta_{40}$  in late amyloidosis stage (Fig. 5B, D and F). Besides, the strongest associations with tau PET for all the biomarkers were found in early Braak ROIs (entorhinal and Braak<sub>III/IV</sub>) in late amyloidosis stage.

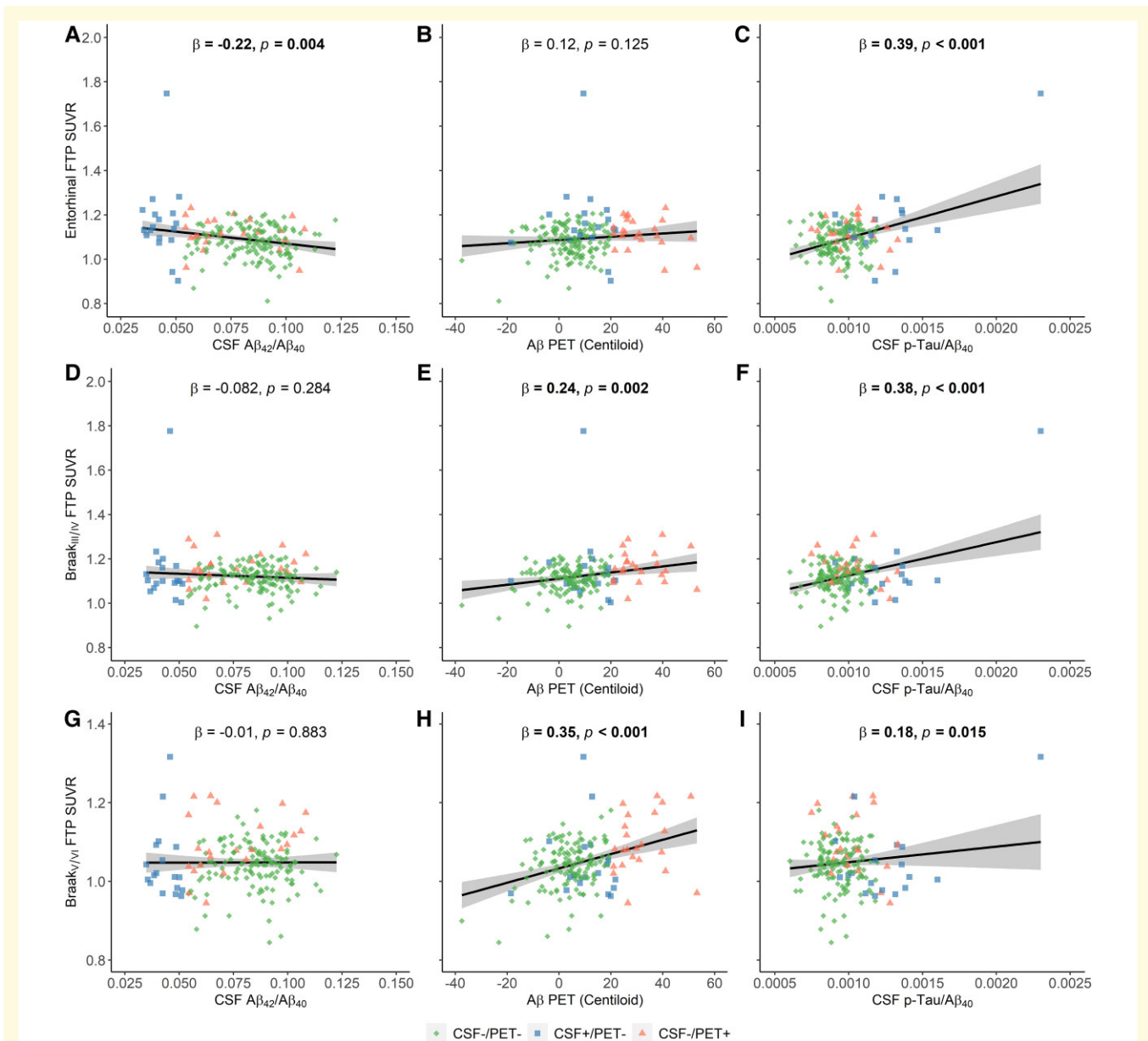


**Figure 3** The association of cortical tau deposition with CSF  $A\beta_{42}/A\beta_{40}$ , A $\beta$  PET and CSF p-Tau/ $A\beta_{40}$  in early amyloidosis stage. The association between entorhinal FTP SUVR and (A) CSF  $A\beta_{42}/A\beta_{40}$ , (B) A $\beta$ -PET(Centiloid) and (C) CSF p-Tau/ $A\beta_{40}$ . The association between Braak<sub>III/IV</sub> FTP SUVR and (D) CSF  $A\beta_{42}/A\beta_{40}$ , (E) A $\beta$ -PET(Centiloid) and (F) CSF p-Tau/ $A\beta_{40}$ . The association between Braak<sub>V/VI</sub> FTP SUVR and (G) CSF  $A\beta_{42}/A\beta_{40}$ , (H) A $\beta$ -PET(Centiloid) and (I) CSF p-Tau/ $A\beta_{40}$ .

After removing two individuals with extremely high entorhinal FTP SUVRs, the significant association between tau PET and CSF p-Tau/ $A\beta_{40}$  in early amyloidosis stage disappeared, whilst the other associations retained (Supplemental Fig. 13). Besides, the results were substantially the same whilst we removed the borderline individuals (Supplemental Fig. 19).

## Discussion

In this study, we investigated the cortical tau deposition measured by tau PET imaging of different amyloidosis stages

defined by CSF  $A\beta_{42}/A\beta_{40}$  and A $\beta$  PET in non-demented elderly adults. Compared to CSF  $A\beta_{42}/A\beta_{40}$  negative and A $\beta$  PET negative (CSF-/PET-) individuals without tau increase in CSF or cortex, we found individuals with abnormal CSF  $A\beta_{42}/A\beta_{40}$  only (CSF+/PET-) showed higher tau in entorhinal but not in Braak<sub>III/IV</sub> and Braak<sub>V/VI</sub>, whereas individuals with abnormal A $\beta$  PET only (CSF-/PET+) had significant tau elevations in Braak<sub>V/VI</sub> but not in entorhinal and Braak<sub>III/IV</sub>. The voxel-wise analyses provided further evidence that lower CSF  $A\beta_{42}/A\beta_{40}$  was associated with higher tau in entorhinal, whilst higher A $\beta$  PET was related to higher tau in Braak<sub>V/VI</sub> ROIs in early amyloidosis stage (CSF+/PET- and CSF-/PET+). In contrast, individuals with

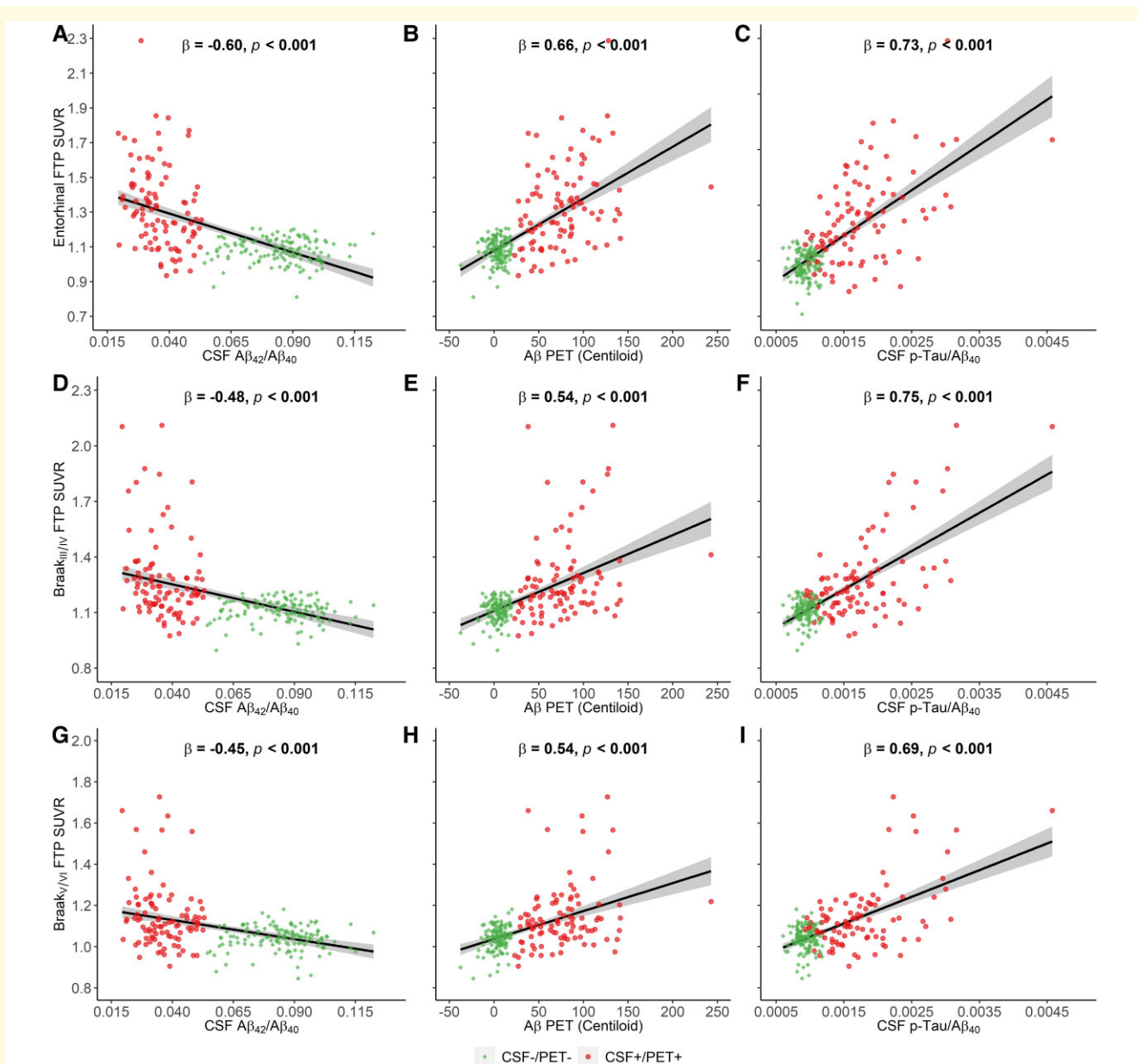


**Figure 4** The association of cortical tau deposition with CSF A $\beta_{42}/A\beta_{40}$ , A $\beta$  PET and CSF p-Tau/A $\beta_{40}$  in late amyloidosis stage. The association of entorhinal FTP SUVR with (A) CSF A $\beta_{42}/A\beta_{40}$ , (B) A $\beta$ -PET(Centiloid), and (C) CSF p-Tau/A $\beta_{40}$ . The association of Braak<sub>III/IV</sub> FTP SUVR with (D) CSF A $\beta_{42}/A\beta_{40}$ , (E) A $\beta$ -PET(Centiloid), and (F) CSF p-Tau/A $\beta_{40}$ . The association of Braak<sub>V/VI</sub> FTP SUVR with (G) CSF A $\beta_{42}/A\beta_{40}$ , (H) A $\beta$ -PET(Centiloid) and (I) CSF p-Tau/A $\beta_{40}$ .

abnormal CSF A $\beta_{42}/A\beta_{40}$  and abnormal A $\beta$  PET (CSF+/PET+) had significant tau elevations in all the Braak ROIs, and both lower CSF A $\beta_{42}/A\beta_{40}$  and higher A $\beta$  PET were correlated with higher tau in entorhinal, Braak<sub>III/IV</sub> and Braak<sub>V/VI</sub> in late amyloidosis stage. These findings provide novel insights into understanding the cortical tau aggregation in different amyloidosis stages of Alzheimer's disease, suggesting CSF A $\beta$  and A $\beta$  PET discordant individuals may have initial tau tangles in distinct cortical regions in early amyloidosis stage of Alzheimer's disease.

In line with previous studies,<sup>7,8,16</sup> we found CSF+/PET- individuals (CSF-first A $\beta$  pathway) and CSF-/PET+

individuals (PET-first A $\beta$  pathway) had similar proportion, and both of them had more A $\beta$  pathology measured by either CSF or PET imaging than the CSF-/PET- individuals, supporting that CSF A $\beta$  and A $\beta$  PET may measure different features of A $\beta$  pathology<sup>7,24,48</sup> and two distinct A $\beta$  pathways<sup>22</sup> exist in early amyloidosis stage of Alzheimer's disease. Furthermore, both CSF+/PET- and CSF-/PET+ individuals had higher CSF p-Tau/A $\beta_{40}$  ratios than the CSF-/PET- individuals, implying that the early abnormal tau increases in CSF<sup>36,49,50</sup> are detectable in early amyloidosis stage. Notably, the CSF+/PET- individuals also showed higher CSF p-Tau/A $\beta_{40}$  ratio than the CSF-/PET+

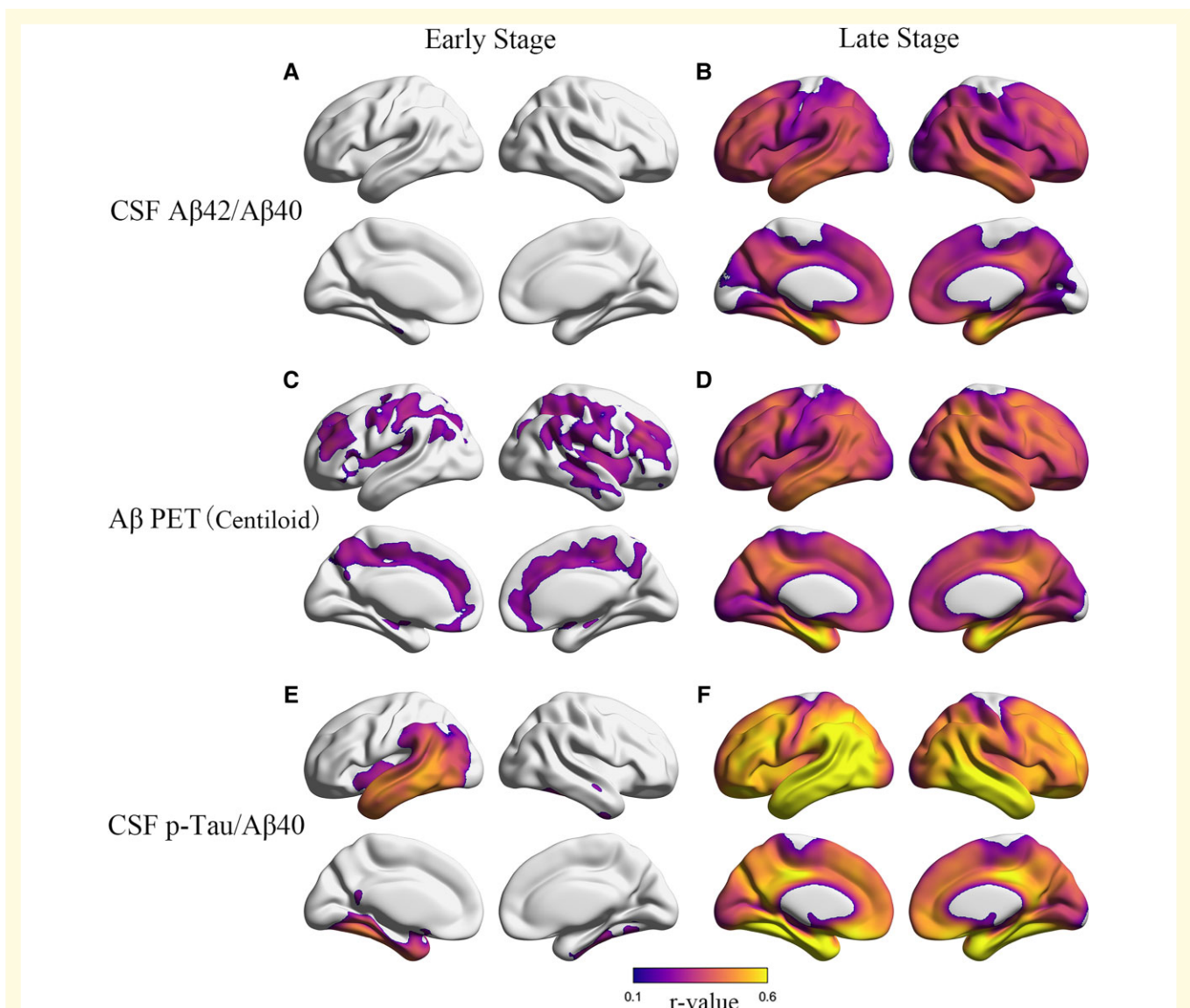


**Figure 5** Voxel-wise analyses of cortical tau with CSF biomarkers and A $\beta$  PET in early and late amyloidosis stages. Cortical regions with significant associations between FTP SUVR and (A) CSF A $\beta_{42}$ /A $\beta_{40}$ , (C) A $\beta$  PET, (E) CSF p-Tau/A $\beta_{40}$  and in early amyloidosis stage. The voxel-wise correlation between CSF A $\beta_{42}$ /A $\beta_{40}$  and FTP tau PET was presented as  $P < 0.005$  at the voxel level without cluster correction. The other voxel-wise correlation results were presented with using a threshold  $P < 0.001$  at the voxel level and with FWE corrected  $P < 0.05$  at the cluster level. Cortical regions with significant associations between FTP SUVR and (B) CSF A $\beta_{42}$ /A $\beta_{40}$ , (D) A $\beta$  PET, (F) CSF p-Tau/A $\beta_{40}$  and in the late amyloidosis stage. Results are shown using a threshold  $P < 0.001$  at the voxel level and with FWE corrected  $P < 0.05$  at the cluster level.

individuals. Together, these findings suggest that the CSF-first A $\beta$  pathway (CSF-/PET-  $\rightarrow$  CSF+/PET-  $\rightarrow$  CSF+/PET+) may have more soluble Alzheimer's disease pathophysiology, which typically present in early stage of Alzheimer's disease,<sup>7,36,49,50</sup> than the PET-first A $\beta$  pathway (CSF-/PET-  $\rightarrow$  CSF-/PET+  $\rightarrow$  CSF+/PET+).

Whilst CSF measurement of p-Tau provides complementary early tau increase,<sup>36,49,50</sup> PET imaging offers spatial information on where tau deposits. Notably, our group<sup>36</sup> and other laboratories<sup>49,50</sup> very recently observed evidence that CSF p-Tau may detect early tau increase than the tau PET imaging, which was also supported by postmortem studies.<sup>51-53</sup>

Importantly, both dichotomous and continuous analyses showed that the CSF-first A $\beta$  pathway had A $\beta$ -related tau increase in entorhinal cortex, which has been regarded as the earliest cortical region of tau aggregation.<sup>38-43</sup> In contrast, the PET-first A $\beta$  pathway showed significant A $\beta$ -related tau increase in Braak<sub>V/VI</sub> but not in entorhinal and Braak<sub>III/IV</sub>. In concordance with our findings, one recent important ADNI study<sup>32</sup> also found that the CSF+/PET- and CSF-/PET+ individuals have numerically (not significant) higher and lower entorhinal tau measured around 5 year post-baseline CSF A $\beta$  and A $\beta$  PET than the CSF-/PET- individuals respectively, although they used CSF A $\beta_{42}$  to define

CSF A $\beta$  status, which may be less reliable than CSF A $\beta_{42}$ /A $\beta_{40}$  used in this study. They also found CSF-/PET+ but not CSF+/PET- individuals had significant tau increase in Braak<sub>V/VI</sub> but not in entorhinal and Braak<sub>III/IV</sub>, which was consistent with our findings. Together with our findings and previous study,<sup>32</sup> it is probably that individuals with PET-first A $\beta$  pathway may not have tau increases in entorhinal and Braak<sub>III/IV</sub> cortical regions due to their lower CSF p-Tau, which plays an important role in tau spreading in cortical regions of early Braak stages (entorhinal and Braak<sub>III/IV</sub>).<sup>36,49,50</sup> The voxel-wise results provide further evidence to support the notion that CSF A $\beta_{42}$ /A $\beta_{40}$  may be related to tau aggregation in entorhinal cortex whereas cortical A $\beta$  burden correlates with elevated tau in cortical regions of Braak<sub>V/VI</sub> stage in early amyloidosis stages. Notably, the CSF-/PET+ individuals had smaller CSF p-Tau/A $\beta_{40}$  ratio than the CSF+/PET- individuals, suggesting we may not be able to use CSF p-Tau biomarker to represent complementary Braak<sub>V/VI</sub> tau increase in CSF-/PET+ individuals.

Our group<sup>7</sup> and other laboratory<sup>11,54</sup> previously observed that CSF+/PET- individuals were accumulating cortical A $\beta$  burden with a similar rate to the CSF+/PET+ individuals, and will become CSF+/PET+ in future. Besides, the CSF-first A $\beta$  pathway has been observed more frequent than the PET-first A $\beta$  pathway according to the previous reports.<sup>9,13-15,17</sup> In this study, we found similar proportion of CSF and PET A $\beta$  discordant groups, but our previous longitudinal analyses<sup>7</sup> also support that CSF A $\beta$  may become abnormal earlier than A $\beta$  PET. Consequently, it is probably that the CSF-first A $\beta$  pathway may represent the typical evolution of Alzheimer's disease which shows Alzheimer's typical tau spreading pattern,<sup>38-43</sup> whilst the PET-first A $\beta$  pathway may have cortical A $\beta$ -burden related hippocampal-sparing elevated tau in early amyloidosis stage of Alzheimer's disease. The Temporal-metaROI (entorhinal, amygdala, parahippocampal, fusiform, inferior temporal and middle temporal)<sup>44</sup> composite regions have been commonly used to detect Alzheimer's-related tau deposition in human brain.<sup>3,55-60</sup> However, our findings suggested that we may not be able to use Temporal-metaROI regions to capture the cortical tau increase in early amyloidosis stage among these individuals who have a PET-first A $\beta$  pathway, implying different cortical regions should be selected to detect early tau increase in early Alzheimer's disease.

In contrast, we found CSF A $\beta$  positive and A $\beta$  PET positive (CSF+/PET+, late amyloidosis stage) individuals showed significant tau increases in all the cortical regions than the control group, and the highest tau elevations were found in the Temporal-metaROI<sup>44</sup> composite regions. Furthermore, the voxel-wise analyses revealed that lower CSF A $\beta_{42}$ /A $\beta_{40}$ , higher A $\beta$  PET, and larger CSF p-Tau/A $\beta_{40}$  ratio were related to significant tau elevations in all the cortical regions and with Temporal-metaROI<sup>44</sup> composite regions showing the strongest association. These findings suggest that it is reasonable to use Temporal-metaROI regions to detect cortical tau increase in CSF and PET A $\beta$  discordant individuals.

## Limitations

This study has several limitations. First, as CSF A $\beta$  and A $\beta$  PET have a very high agreement, the sample sizes of the discordant CSF/PET A $\beta$  groups with concurrent tau PET imaging were relatively small and the results need to be replicated in a larger cohort. To the best of our knowledge, there is currently no larger cohort available with the measurements needed for this analysis. Second, the ADNI participants overall are a highly selected sample, recruited to reflect the exclusionary criteria and types of individuals likely to participate in clinical trials; thus, it would be extremely useful to validate these findings in other aging cohorts. Third, our analyses were limited to cross-sectional PET measured with FTP, which may need to be replicated using longitudinal data and other PET ligands. Fourth, the threshold of CSF A $\beta_{42}$ /A $\beta_{40}$  was defined on the basis of the ADNI database, which requires validation with other databases.

## Conclusion

In conclusions, we found that CSF and PET A $\beta$  discordant individuals have distinct cortical tau deposition patterns in non-demented elderly adults. Recent studies<sup>61-64</sup> suggest that Alzheimer's disease may have distinct biological features of tau spreading patterns, which are important for explaining the heterogeneity of tau-related neurodegeneration and cognitive decline and the design of anti-tau clinical trials. Our findings are useful for understanding the subtypes of tau spreading patterns in Alzheimer's disease and provide novel reference for cortical tau detection in individuals who are at early amyloidosis stage.

## Acknowledgements

The authors would like to thank all the ADNI participants and staff for their contributions to data acquisition. The Data collection and sharing for this project was funded by the Alzheimer's Disease Neuroimaging Initiative (ADNI) (National Institutes of Health Grant U01 AG024904) and DOD ADNI (Department of Defense award number W81XWH-12-2-0012). ADNI is funded by the National Institute on Aging, the National Institute of Biomedical Imaging and Bioengineering and through generous contributions from the following: AbbVie, Alzheimer's Association; Alzheimer's Drug Discovery Foundation; Araclon Biotech; BioClinica, Inc.; Biogen; Bristol-Myers Squibb Company; CereSpir, Inc.; Eisai Inc.; Elan Pharmaceuticals, Inc.; Eli Lilly and Company; EuroImmun; F. Hoffmann-La Roche Ltd and its affiliated company Genentech, Inc.; Fujirebio; GE Healthcare; IXICO Ltd.; Janssen Alzheimer Immunotherapy Research & Development, LLC.; Johnson & Johnson Pharmaceutical Research & Development LLC.; Lumosity; Lundbeck; Merck & Co., Inc.; Meso Scale Diagnostics, LLC.; NeuroRx Research; Neurotrack

Technologies; Novartis Pharmaceuticals Corporation; Pfizer Inc.; Piramal Imaging; Servier; Takeda Pharmaceutical Company; and Transition Therapeutics. The Canadian Institutes of Health Research is providing funds to support ADNI clinical sites in Canada. Private sector contributions are facilitated by the Foundation for the National Institutes of Health ([www.fnih.org](http://www.fnih.org)). The grantee organization is the Northern California Institute for Research and Education, and the study is coordinated by the Alzheimer's Disease Cooperative Study at the University of California, San Diego. ADNI data are disseminated by the Laboratory for Neuro Imaging at the University of Southern California.

## Funding

This work was supported by the National Natural Science Foundation of China (82171197) and Shenzhen Bay Laboratory Open Project (SZBL2020090501014).

## Competing interests

T.G. services in Alzheimer's Association as the ISTAART 'PIA to Elevate Early Career Researchers (PEERs)' Asia lead. The remaining authors reported no competing interests.

## Supplementary material

Supplementary material is available at *Brain Communications* online.

## References

- McKhann GM, Knopman DS, Chertkow H, et al. The diagnosis of dementia due to Alzheimer's disease: Recommendations from the National Institute on Aging-Alzheimer's Association workgroups on diagnostic guidelines for Alzheimer's disease. *Alzheimer's Dement* 2011;7(3):263–269.
- Jack CR, Bennett DA, Blennow K, et al. NIA-AA research framework: Toward a biological definition of Alzheimer's disease. *Alzheimer's Dement* 2018;14(4):535–562.
- Guo T, Korman D, Baker SL, Landau SM, Jagust WJ. Longitudinal cognitive and biomarker measurements support a unidirectional pathway in Alzheimer's disease pathophysiology. *Biol Psychiatry* 2021;89(8):786–794.
- Guo T, Brendel M, Grimmer T, Rominger A, Yakushev I. Predicting regional pattern of longitudinal  $\beta$ -amyloid accumulation by baseline PET. *J Nucl Med* 2017;58(4):639–645.
- Guo T, Dukart J, Brendel M, Rominger A, Grimmer T, Yakushev I. Rate of  $\beta$ -amyloid accumulation varies with baseline amyloid burden: Implications for anti-amyloid drug trials. *Alzheimer's Dement* 2018;14(11):1387–1396.
- Guo T, Landau SM, Jagust WJ. Detecting earlier stages of amyloid deposition using PET in cognitively normal elderly adults. *Neurology* 2020;94(14):e1512–e1524.
- Guo T, Shaw LM, Trojanowski JQ, Jagust WJ, Landau SM. Association of CSF A $\beta$ , amyloid PET, and cognition in cognitively unimpaired elderly adults. *Neurology* 2020;95(15):e2075–e2085.
- Pannee J, Portelius E, Minthon L, et al. Reference measurement procedure for CSF amyloid beta (A $\beta$ )<sub>1–42</sub> and the CSF A $\beta$ <sub>1–42</sub>/A $\beta$ <sub>1–40</sub> ratio – a cross-validation study against amyloid PET. *J Neurochem* 2016;139(4):651–658.
- Janelidze S, Zetterberg H, Mattsson N, et al. CSF A $\beta$ <sub>42</sub>/A $\beta$ <sub>40</sub> and A $\beta$ <sub>42</sub>/A $\beta$ <sub>38</sub> ratios: Better diagnostic markers of Alzheimer disease. *Ann Clin Transl Neurol* 2016;3(3):154–165.
- Reimand J, de Wilde A, Teunissen CE, et al. PET and CSF amyloid- $\beta$  status are differently predicted by patient features: Information from discordant cases. *Alzheimers Res Ther* 2019;11(1):100.
- Palmqvist S, Mattsson N, Hansson O. Cerebrospinal fluid analysis detects cerebral amyloid- $\beta$  accumulation earlier than positron emission tomography. *Brain* 2016;139(4):1226–1236.
- Reimand J, Boon BDC, Collij LE, et al. Amyloid- $\beta$  PET and CSF in an autopsy-confirmed cohort. *Ann Clin Transl Neurol* 2020;7(11):2150–2160.
- Leuzy A, Chiotis K, Hasselbalch SG, et al. Pittsburgh compound B imaging and cerebrospinal fluid amyloid- $\beta$  in a multi-centre European memory clinic study. *Brain* 2016;139(9):2540–2553.
- Lewczuk P, Matzen A, Blennow K, et al. Cerebrospinal fluid A $\beta$ <sub>42</sub>/40 corresponds better than A $\beta$ <sub>42</sub> to amyloid PET in Alzheimer's disease. *J Alzheimer's Dis* 2017;55(2):813–822.
- Janelidze S, Pannee J, Mikulskis A, et al. Concordance between different amyloid immunoassays and visual amyloid positron emission tomographic assessment. *JAMA Neurol* 2017;74(12):1492–1501.
- Niemantsverdriet E, Ottoy J, Somers C, et al. The cerebrospinal fluid A $\beta$ <sub>1–42</sub>/A $\beta$ <sub>1–40</sub> ratio improves concordance with amyloid-PET for diagnosing Alzheimer's disease in a clinical setting. *J Alzheimer's Dis* 2017;60(2):561–576.
- Schindler SE, Gray JD, Gordon BA, et al. Cerebrospinal fluid biomarkers measured by Elecsys assays compared to amyloid imaging. *Alzheimer's Dement* 2018;14(11):1460–1469.
- Adamczuk K, Schaeverbeke J, Vanderstichele HMJ, et al. Diagnostic value of cerebrospinal fluid A $\beta$  ratios in preclinical Alzheimer's disease. *Alzheimers Res Ther* 2015;7(1):75.
- Doecke JD, Ward L, Burnham SC, et al. Elecsys CSF biomarker immunoassays demonstrate concordance with amyloid-PET imaging. *Alzheimers Res Ther* 2020;12(1):36.
- de Wilde A, Reimand J, Teunissen CE, et al. Discordant amyloid- $\beta$  PET and CSF biomarkers and its clinical consequences. *Alzheimers Res Ther* 2019;11(1):78.
- Alcolea D, Pegueroles J, Muñoz L, et al. Agreement of amyloid PET and CSF biomarkers for Alzheimer's disease on Lumipulse. *Ann Clin Transl Neurol* 2019;6(9):1815–1824.
- Sala A, Nordberg A, Rodriguez-Vieitez E. Longitudinal pathways of cerebrospinal fluid and positron emission tomography biomarkers of amyloid- $\beta$  positivity. *Mol Psychiatry* 2021;26(10):5864–5874.
- Zwan MD, Rinne JO, Hasselbalch SG, et al. Use of amyloid-PET to determine cutpoints for CSF markers. *Neurology* 2016;86(1):50–58.
- Mattsson N, Insel PS, Donohue M, et al. Independent information from cerebrospinal fluid amyloid- $\beta$  and florbetapir imaging in Alzheimer's disease. *Brain* 2015;138(3):772–783.
- Toledo JB, Bjerke M, Da X, et al. Nonlinear association between Cerebrospinal fluid and florbetapir F-18  $\beta$ -amyloid measures across the spectrum of Alzheimer disease. *JAMA Neurol* 2015;72(5):571–581.
- Vos SJB, Gordon BA, Su Y, et al. NIA-AA staging of preclinical Alzheimer disease: Discordance and concordance of CSF and imaging biomarkers. *Neurobiol Aging* 2016;44:1–8.
- Hansson O, Seibyl J, Stomrud E, et al. CSF biomarkers of Alzheimer's disease concord with amyloid- $\beta$  PET and predict clinical progression: A study of fully automated immunoassays in

- BioFINDER and ADNI cohorts. *Alzheimer's Dement* 2018;14(11):1470–1481.
28. Koivunen J, Pirttilä T, Kemppainen N, *et al.* PET amyloid ligand [<sup>11</sup>C]PIB uptake and cerebrospinal fluid  $\beta$ -amyloid in mild cognitive impairment. *Dement Geriatr Cogn Disord* 2008;26(4):378–383.
  29. Fagan AM, Mintun MA, Shah AR, *et al.* Cerebrospinal fluid tau and ptau<sub>181</sub> increase with cortical amyloid deposition in cognitively normal individuals: Implications for future clinical trials of Alzheimer's disease. *EMBO Mol Med* 2009;1(8-9):371–380.
  30. Landau SM, Lu M, Joshi AD, *et al.* Comparing positron emission tomography imaging and cerebrospinal fluid measurements of  $\beta$ -amyloid. *Ann Neurol* 2013;74(6):826–836.
  31. Zwan M, van Harten A, Ossenkoppele R, *et al.* Concordance between cerebrospinal fluid biomarkers and [11C]PIB PET in a memory clinic cohort. *J Alzheimer's Dis* 2014;41(3):801–807.
  32. Reimand J, Collij L, Scheltens P, Bouwman F, Ossenkoppele R. Association of amyloid- $\beta$  CSF/PET discordance and tau load 5 years later. *Neurology* 2020;95(19):e2648–e2657.
  33. Leal SL, Lockhart SN, Maass A, Bell RK, Jagust WJ. Subthreshold amyloid predicts tau deposition in aging. *J Neurosci* 2018;38(19):4482–4489.
  34. Tosun D, Landau S, Aisen PS, *et al.* Association between tau deposition and antecedent amyloid- $\beta$  accumulation rates in normal and early symptomatic individuals. *Brain* 2017;140(5):1499–1512.
  35. Hanseeuw BJ, Betensky RA, Jacobs HIL, *et al.* Association of amyloid and tau with cognition in preclinical Alzheimer disease. *JAMA Neurol* 2019;76(8):915.
  36. Guo T, Korman D, La Joie R, *et al.* Normalization of CSF pTau measurement by A $\beta$ 40 improves its performance as a biomarker of Alzheimer's disease. *Alzheimers Res Ther* 2020;12(1):97.
  37. Knopman DS, Lundt ES, Therneau TM, *et al.* Association of initial  $\beta$ -Amyloid levels with subsequent flortaucipir positron emission tomography changes in persons without cognitive impairment. *JAMA Neurol* 2021;78(2):217.
  38. Braak H, Braak E. Neuropathological staging of Alzheimer-related changes. *Acta Neuropathol* 1991;82(4):239–259.
  39. Schöll M, Lockhart SN, Schonhaut DR, *et al.* PET imaging of tau deposition in the aging human brain. *Neuron* 2016;89(5):971–982.
  40. Sanchez JS, Becker JA, Jacobs HIL, *et al.* The cortical origin and initial spread of medial temporal tauopathy in Alzheimer's disease assessed with positron emission tomography. *Sci Transl Med* 2021;13(577):eabc0655.
  41. Cho H, Choi JY, Hwang MS, *et al.* In vivo cortical spreading pattern of tau and amyloid in the Alzheimer disease spectrum. *Ann Neurol* 2016;80(2):247–258.
  42. Doré V, Krishnadas N, Bourgeat P, *et al.* Relationship between amyloid and tau levels and its impact on tau spreading. *Eur J Nucl Med Mol Imaging* 2021;48(7):2225–2232.
  43. Pascoal TA, Therriault J, Benedet AL, *et al.* 18F-MK-6240 PET for early and late detection of neurofibrillary tangles. *Brain* 2020;143(9):2818–2830.
  44. Jack CR, Wiste HJ, Weigand SD, *et al.* Defining imaging biomarker cut points for brain aging and Alzheimer's disease. *Alzheimer's Dement* 2017;13(3):205–216.
  45. Desikan RS, Ségonne F, Fischl B, *et al.* An automated labeling system for subdividing the human cerebral cortex on MRI scans into gyral based regions of interest. *Neuroimage* 2006;31(3):968–980.
  46. Landau SM, Fero A, Baker SL, *et al.* Measurement of longitudinal  $\beta$ -amyloid change with <sup>18</sup>F-florbetapir PET and standardized uptake value ratios. *J Nucl Med* 2015;56(4):567–574.
  47. Maass A, Landau S, Baker SL, *et al.* Comparison of multiple tau-PET measures as biomarkers in aging and Alzheimer's disease. *Neuroimage* 2017;157:448–463.
  48. Cohen AD, Landau SM, Snitz BE, Klunk WE, Blennow K, Zetterberg H. Fluid and PET biomarkers for amyloid pathology in Alzheimer's disease. *Mol Cell Neurosci* 2019;97(7):3–17.
  49. Mattsson-Carlgen N, Andersson E, Janelidze S, *et al.* A $\beta$  deposition is associated with increases in soluble and phosphorylated tau that precede a positive Tau PET in Alzheimer's disease. *Sci Adv* 2020;6(16):eaaz2387.
  50. Meyer P-F, Pichet Binette A, Gonneaud J, Breitner JCS, Villeneuve S. Characterization of Alzheimer disease biomarker discrepancies using cerebrospinal fluid phosphorylated Tau and AV1451 positron emission tomography. *JAMA Neurol* 2020;77(4):508.
  51. Day GS, Gordon BA, Perrin RJ, *et al.* In vivo [<sup>18</sup>F]-AV-1451 tau-PET imaging in sporadic Creutzfeldt-Jakob disease. *Neurology* 2018;90(10):e896–e906.
  52. Fleisher AS, Pontecorvo MJ, Devous MD, *et al.* Positron emission tomography imaging with [<sup>18</sup>F]flortaucipir and postmortem assessment of Alzheimer disease neuropathologic changes. *JAMA Neurol* 2020;77(7):829.
  53. Chen CD, Holden TR, Gordon BA, *et al.* Ante- and postmortem tau in autosomal dominant and late-onset Alzheimer's disease. *Ann Clin Transl Neurol* 2020;7(12):2475–2480.
  54. Palmqvist S, Schöll M, Strandberg O, *et al.* Earliest accumulation of  $\beta$ -amyloid occurs within the default-mode network and concurrently affects brain connectivity. *Nat Commun* 2017;8(1):1214.
  55. Jack CR, Wiste HJ, Schwarz CG, *et al.* Longitudinal tau PET in aging and Alzheimer's disease. *Brain* 2018;141(5):1517–1528.
  56. Jack CR, Wiste HJ, Therneau TM, *et al.* Associations of Amyloid, Tau, and Neurodegeneration biomarker profiles with rates of memory decline among individuals without dementia. *JAMA* 2019;321(23):2316.
  57. Jack CR, Wiste HJ, Botha H, *et al.* The bivariate distribution of amyloid- $\beta$  and tau: Relationship with established neurocognitive clinical syndromes. *Brain* 2019;142(10):3230–3242.
  58. Park J-C, Han S-H, Yi D, *et al.* Plasma tau/amyloid- $\beta$ 1–42 ratio predicts brain tau deposition and neurodegeneration in Alzheimer's disease. *Brain* 2019;142(3):771–786.
  59. Graff-Radford J, Arenaza-Urquijo EM, Knopman DS, *et al.* White matter hyperintensities: Relationship to amyloid and tau burden. *Brain* 2019;142(8):2483–2491.
  60. Botha H, Mantyh WG, Graff-Radford J, *et al.* Tau-negative amnesic dementia masquerading as Alzheimer disease dementia. *Neurology* 2018;90(11):e940–e946.
  61. Dujardin S, Commins C, Lathuiliere A, *et al.* Tau molecular diversity contributes to clinical heterogeneity in Alzheimer's disease. *Nat Med* 2020;26(8):1256–1263.
  62. Vogel JW, Young AL, Oxtoby NP, *et al.* Four distinct trajectories of tau deposition identified in Alzheimer's disease. *Nat Med* 2021;27(5):871–881.
  63. Ossenkoppele R, Lyoo CH, Sudre CH, *et al.* Distinct tau PET patterns in atrophy-defined subtypes of Alzheimer's disease. *Alzheimer's Dement* 2020;16(2):335–344.
  64. Therriault J, Pascoal TA, Savard M, *et al.* Topographic distribution of Amyloid- $\beta$ , Tau, and Atrophy in patients with behavioral/dysexecutive Alzheimer disease. *Neurology* 2021;96(1):e81–e92.